HHS Public Access

Author manuscript

Colloids Surf A Physicochem Eng Asp. Author manuscript; available in PMC 2022 September 20.

Published in final edited form as:

Colloids Surf A Physicochem Eng Asp. 2021 September 20; 625: . doi:10.1016/j.colsurfa.2021.126810.

A High-adhesion Binding Strategy for Silica Nanoparticle-based Superhydrophobic Coatings

Xiaoxiao Zhao, **Michael C. Murphy***

Center for BioModular Multiscale Systems for Precision Medicine, Department of Mechanical & Industrial Engineering, Louisiana State University, Baton Rouge, LA 70803, United States

Abstract

One of the long-standing problems for the nanoparticle-based liquid-repellent coatings is their poor adhesion to substrates. For polymers of low glass transition temperature, it is highly desirable to have low temperature coating strategy to fabricate robust superhydrophobic films. Here, we report a facile method for fabricating robust, transparent, superhydrophobic films on polymer substrates. A mixture of silica particles and silica-based oligomers was spin coated on polymer substrates, followed by oxygen plasma treatment and vapor deposition of 1H,1H,2H,2H-Perfluorodecyltriethoxysilane (FDTS). The resulting superhydrophobic surface has a static contact angle at 160° and contact angle hysteresis lower than 5°. This study provides a practical solution to improve the adhesion of superhydrophobic films on polymer substrates in ambient conditions.

Graphical Abstract

* murphy@lsu.edu .

Conflict of Interest

The authors declare no conflict of interest.

Declaration of interests

The authors declare that they have no known competing financial interests or personal relationships that could have appeared to influence the work reported in this paper.

Credit Author Statement

Xiaoxiao Zhao: Conceptualization, Methodology, Writing.

Michael C. Murphy: Review & editing.

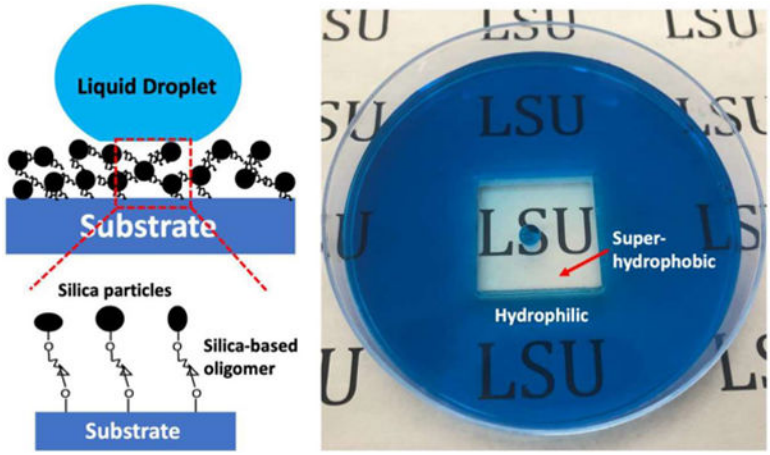

Keywords

Superhydrophobic; polymer substrate; nanoparticles; polymer binders

1. Introduction

Superhydrophobic surfaces have attracted significant interest for their unique self-cleaning properties. Increasing surface roughness and lowering surface free energy are usually combined to fabricate superhydrophobic surfaces. First, superhydrophobicity cannot be achieved without surface roughness. For example, CF_3-terminated, $C_{20}F_{42}$ molecules grafted, ultra-smooth surface has the lowest surface free energy of 6.7 mJ/m^2 while only achieving an average water contact angle (CA) of 119°.[1,2] Thus, silica nanoparticles have been widely used to introduce surface roughness for liquid-repellent coatings. Second, lowering surface free energy involves covalent grafting of fluorocarbon or hydrocarbon long chain molecules on solid substrates. The surface free energy increases in the order $-CF_3$ < $-CF_2H$ < $-CF_2$ < $-CH_3$ < $-CH_2-$, with $-CF_3$ providing the highest superhydrophobicity.[3] Meanwhile, the longer molecular chain length is more effective in lowering the surface free energy. For example, Liu et al.[4] reported the water CA of treated cotton fabric increases in the order $-C_3F_4H_3$ < $-C_4F_6H_3$ < $-C_5F_8H_3$ < $-C_7F_{13}H_2$, since longer molecular chain increased fluorine converge on surface and thus improved surface superhydrophobicity. Therefore, it is favorable to enhance the surface roughness and grafting high molecular weight fluorine for an increased liquid repellency.

Generating surface porosity is a straightforward way to enhance surface roughness and therefore superhydrophobicity. Erbil et al.[5] used p-xylene to dissolve isotactic polypropylene (i-PP) at 130 °C and then casted dissolved solution onto various substrates to obtain porous gel-like coating structures with water CA of 160°. Tadanaga et al.[6] created flowerlike surface porosity with roughness of 20–50 nm by immersing boehmite (AlOOH) gel films in boiling water for a variety of times (0–10 min). The obtained crystallized films were hydrophobilized to achieve water CA of 165° and optical transmittance higher than 92%. However, Chan et al.[7] reported boiling water may cause hydrolysis of Si-O-C bonds between oxygen plasma treated polymer substrates and silica-based coatings, resulting in

coatings with poor adhesion and cracking. Nakajima et al.[8] prepared suspension by mixing 30 nm boehmite or 20 nm silica with aluminum acetylacetonate ($Al(C_5H_7O_2)_3$) at 193 °C. After repeatedly spin coating on glass substrate at 1000 rpm for 10 s and calcination at 500 °C for 20 s, the aluminum acetylacetonate was removed and left multiple 100–300 nm pores on the coating surface. In addition to surface porosity, transparency property has wide potential applications in windows, digital screens, solar panels. Reducing the size of surface structure is a common approach to improve optical transmittance while maintaining sufficient surface roughness for superhydrophobicity.[9–11] However, further lowering the structure size below 20 nm may lose its superhydrophobicity due to the reduced surface roughness and the effect of long-range forces.[12,13] Also, chemical binders usually smoothen the surface by filling the porosity of the silica particle films. Thus, the adhesion of silica coating and the coating porosity are usually considered as competing properties.

Several literature papers reported the improvement of silica coatings adhesion without compromising their porosities, thereby ensuring the hierarchical roughness of superhydrophobic surfaces. For example, electrostatic force has been commonly employed to assist the adherence of silica particles to substrates. This is achieved by treating the substrates with positive charge to attract the intrinsically negatively charged silica particles.[14–16] However, this electrostatic interaction is non-covalent and thus leading to a weak anchoring of silica particles. As a result, the silica particles could be simply rinsed away by a few cycles of droplet impacts. To further improve interparticle adhesion, amine (e.g. 3-aminopropyltriethoxysilane) and epoxy (e.g., 3-glycidoxypropyltrimethoxysilane) functionalization of silica particles have been extensively studied to form covalent attachments among particles as well as with substrates [17–20]. However, the rigid silica spheres only formed point contact with each other, leading to a reduced adhesion strength. Also, the covalently bonded silica particles could be easily detached after a few minutes of sonication. To improve covalent attachment area, polymer binders are commonly incorporated to form connecting bridges between silica nanoparticles.[21–24] However, the agglomeration of silica particles usually occurs due to the presence of highly adhesive polymers in the colloidal coating solution. This leads to a non-uniform particle coverage and restricts its potential applications, especially in area demanding high optical transmittance such as windshields, optical lenses, and solar cell panels.[25,26] Although high temperature sintering (360–1100 °C) has shown its effectiveness in creating robust and stable silica coating films,[27–29] this method is not applicable to polymer substrates owing to their relatively low glass transition temperatures (e.g., 105 °C for PMMA). Therefore, it is favorable to incorporate a low temperature, uniform coating approach to increase the silica adhesion while simultaneously enabling superhydrophobicity.

In this study, we dispersed inorganic silica particles in silica-based oligomer solutions to form hybrid silica-silica networks linked by covalent bond. The silica-based oligomer contains abundant hydroxyl groups to form Si-O-Si bonds between coatings and substrates with improved adhesion strength. The liquid repellency, mechanical durability, and optical transparency of the surface were investigated. After solvent evaporation, it generates porosities on coating films with improved surface roughness. We coated different size combination of silica particles and compared their corresponding surface uniformity, transparency, and superhydrophobicity.

2. Experimental

2.1 Materials

Poly(methyl methacrylate) (PMMA) (Cope Plastics, 100×100 mm surface area, 0.75 mm thick) was used as spin-coating substrates. Commercial Scotch tape was provided by Scotch™ Multi-Task Tape, 3 M (St. Paul, MN). Anhydrous ethanol was obtained from Decon Laboratories (200 proof). Tetraethyl orthosilicate (TEOS) was supplied by Acros Organics (98%). Ammonia was purchased from VWR International (28–30%). Hydrochloric acid (HCl) and sodium hydroxide (NaOH) were purchased from VWR International (36.5–38%). Perfluorodecyltrichlorosilane (FDTS) was obtained from Gelest, Inc. Methylene Blue was purchased from Aldon Corporation (Avon, NY).

2.2 Synthesis of silica particles

Silica particles of 70 nm, 400 nm and 650 nm were synthesized using Stöber method[30]. For 70 nm nanoparticles, 5 ml TEOS was added dropwise to a flask containing a mixture of 200 ml ethanol and 10 ml ammonia. The solution was magnetically stirred at 600 rpm for 18 h at room temperature. The obtained 70 nm nanoparticles were centrifuged and vacuum-dried overnight. As shown in Table 1, 400 nm and 650 nm nanoparticles were prepared with the same procedure by varying the concentration of ammonia and TEOS.

2.3 Preparation of superhydrophobic surfaces

Silica-oligomer hybrid films were spin coated onto the PMMA substrates. The spin coating mixture composed of silica particles and suspension of silica-based oligomers. The suspension of silica-based oligomers was prepared by mixing 1 g TEOS, 1 g HCl, 10 g ethanol and then stirring at 700 rpm for 90 min at 60 °C. The PMMA substrate was then oxygen plasma (30 W, 0.15 Torr, Harrick Plasma PDC-32G) treated for 30 s before spin coating. The spin coating speed for 70 nm, 400/70 nm and 650/70 nm films was 1000 rpm, 750 rpm and 500 rpm, respectively. The concentration of silica particles was optimized and listed in Table S1.

The spin coated substrates were put in 60 °C oven for 12 h for solvent evaporation. To lower the overall surface energy, the spin coated substrates were first oxygen plasma treated (30 W, 0.15 Torr, Harrick Plasma PDC-32G, Ithaca, NY) for 3 min, and then 0.1 ml FDTS was placed 50 mm from the substrates in a vacuum desiccator (30 min) to allow vapor deposition and covalent grafting. The vaporized FDTS molecules spontaneous formed covalent bonding on the hydroxyl functionalized substrates, without requiring ion bombardment (e.g., Plasma-Enhanced Chemical Vapor Deposition) to create reactive radicals.[31–33]

2.4 Optical transmittance measurements

The optical transmittance measurements were conducted using a Thermo Electron Helios UV–Vis spectrophotometer (Thermo Electron Corp., Madison, WI). The transmittance percentage of silica nanoparticle coatings was calculated by considering the uncoated PMMA substrate as 100% in the visible wavelength range (400–700 nm).

2.5 Characterization

The morphology of the silica-oligomer hybrid film was analysed using a Field Emission Gun Scanning Electron Microscope (FEG-SEM, The quanta 3D DualBeam). Prior to SEM imaging, the superhydrophobic samples were sputtered with a layer of 10 nm platinum (EMS550X sputter coater) to improve surface conductivity and reduce charging effect. The static CAs and contact angle hysteresis (CAH) were measured using a VCR Optima goniometer (AST Products, Inc.) installed with a droplet shape software (VCA Optima XE). Static CAs were measured by a sessile drop of 5 μL water droplet onto sample surfaces. CAH was measured as the difference of the advancing and receding CAs, which is conducted by adding and removing liquid from the PMMA coating surface, and the volume of the liquid droplet was 10 μL. Five different positions on each sample were measured.

3. Results and discussion

The mechanism and procedures of silica-based oligomers to bind silica nanoparticles was illustrated in Figure 1. The silica-based TEOS was mixed with hydrochloric acid as catalyst in an ethanol solution. In the environment of insufficient water, the hydrolyzed TEOS is prone to form short chain, low molecular weight silica-based oligomer with reactive hydroxyl groups. For details, PMMA substrate was treated with oxygen plasma to generate abundant hydroxyl groups. The silica-based TEOS oligomers solution was in strong acidic condition, and the synthesized silica particles also have large amount of hydroxyl groups. Next, a mixture of silica-based oligomers and silica particles was spin coated on PMMA substrate. After heat treatment, silica-based oligomers formed Si-O-Si bonds between coatings and substrates to improve surface adhesion.[34] Additionally, the heat treatment also generated porosities on coating films to improve surface roughness.

To investigate the effect of silica size on the liquid repellency of the coating surfaces, three diameters of silica nanoparticles was synthesized (Table 1, Figure S1) and spin coated onto the PMMA substrates. We selected three combinations of silica nanoparticles: 70 nm, 400/70 nm, and 650/70 nm. The introduction of dual-sized silica nanoparticles is to investigate the effect of hierarchical structures on the surface superhydrophobicity. Figure 2 shows the surface morphology of these three films. The 650/70 nm film maintains a high water CA at 163° (CAH = 2°) due to its micro- and nano-hierarchical surface structures (Figure 2a), while showing compromised optical transparency (Figure 2d and Figure 3a). The 70 nm film has the highest coating uniformness and optical transparency, while exhibiting the lowest water CA at 158° (CAH = 3°, Figure 2c). For this concern, the 400/70 nm film with water CA at 161° (CAH = 2°) is best qualified as uniform, transparent, superhydrophobic coating on PMMA substrates (Figure 2b).

For all the three silica particle films, the spin coating speed was adjusted to be sufficiently high to avoid particle agglomeration, while not too high to cause inadequate surface coverage of nanoparticles. For larger silica particles, it requires a lower spin coating speed to create thicker films for sufficient surface coverage. However, the large 650 nm particles lead to unavoidable particle agglomeration. Further increasing the spin coating speed of 650/70 nm film to 1000 rpm would cause insufficient surface coverage (Figure S2a)., and further resulting in a dramatic decrease of water contact angles. Conversely, significantly

reducing the spin coating speed to 250 rpm would otherwise cause an even thicker and less transparent coating film (Figure S2b). Similarly, we observed the same effect of spin coating speed on the coating films of 70 nm (Figure S2c–d) and 400/70 nm (Figure S2e–f).

It has shown that the smaller surface structures and thinner coating films would enable higher optical transparency in visible light wavelength of 400–700 nm.[35] Thus, we expect that the 70 nm silica nanoparticles with smaller surface features would result in higher optical transparency. In addition, silica nanoparticle is a great material candidate for transparent coatings due to its low refractive index (n=1.5[36]) and short band gap wavelength with low absorption (138 nm[37]). As expected, we observed a decreasing trend of optical transparency with increasing silica nanoparticle size (Figure 3a).

As the 400/70 nm coating film meets the criteria of being uniform, transparent, superhydrophobic among the three coatings, we further studied its repellency to liquids of various surface tensions. The liquid mixture with surface tension of 72.75, 56.41, 48.14, 42.72, 38.56, 33.53, and 28.51 mN/m were obtained by adding 0%, 5%, 10%, 15%, 20%, 30%. 50% of ethanol in DI water, respectively. This was based on the surface tension results from Vazquez, et al. to formulate mixtures of ethanol and water.[38] We have shown that the surface remains highly liquid repellent (static CA > 120°, CAH < 30°) for surface tension greater than 38.56 mN/m (Figure 3b), as measured by the VCR Optima goniometer using the sessile drop technique. Therefore, we expect that the 400/70 nm film may become omniphobic or even superomniphobic by introducing re-entrant structures prior to the nanoparticle deposition in the future.

To study the adhesion strength of the silica nanoparticles to the PMMA substrates, we conducted tape peeling tests on all the three silica coating films. In a typical tape peeling test, a pressure of 100 kPa was exerted on the Scotch tape to get a conformal contact with the sample surfaces, followed by immediately peeling off. Note that all the tape peeling tests were conducted before the deposition of FDTS. This is because the low surface energy FDTS would otherwise make the sample surfaces less adhesive to the Scotch tape. Except for tape peeling, all other sample analysis and durability tests were performed after the FDTS deposition. As shown in Figure 4c, the silica nanoparticles remained adhered on the PMMA surface after the tape peeling tests, owing to the binding of the silica-based oligomers. In contrast, without any binders to the silica particles, we have previously shown that the coating films were almost particle free after tape peeling.[9] Further, we tested the adhesion force of the silica coating using a standard cross-cut tape test (Figure 3d–e, ISO-2049:2013).[39] Similarly, the 400/70 nm coating film remained superhydrophobic (CA > 150°, CAH < 10°) after 30 cycles of standard tape peeling tests (Figure 3f). Further, the superhydrophobicity of 400/70 nm coated PMMA substrate was also tested by measuring water contact angles after bending motion (Figure 3g). Superhydrophobicity was well maintained after 50 bending cycles with bending radius of 10 mm (Figure 3h). Additionally, After exposure to tap water jet with pressure around 100 kPa for 3 min, the 400/70 nm silica coated PMMA substrate exhibited the same liquid repellency (Figure S3).

Corrosion resistance is essential for superhydrophobic applications in outdoor environment. The corrosion test was conducted by immersing superhydrophobic PMMA substrate (coated

with 400/70 nm films) in HCl and NaOH solutions for 24 h with PH = 2 and 12, respectively. Additionally, both HCl and NaOH solutions were magnetically stirred to simulate the surface corrosion resistance in the practical liquid flowing state. As shown in Figure 4a–b, the superhydrophobic sample surfaces maintained high CA (> 150°) and low CAH (< 10°) after 24 h of immersion in both acidic and basic solutions under liquid flowing state. To further demonstrate the corrosion resistance of the coating surfaces, we deposited silica particles in the centre square of a petri dish to make this area superhydrophobic, while leaving the rest area in pristine hydrophilic state. After pouring acidic or basic solutions (dyed with methylene blue) into the petri dish, we found that the center superhydrophobic area maintained liquid-free for 7 days (Figure 4c and Figure S4).

4. Conclusions

To summarize, we fabricated uniform, transparent, superhydrophobic surfaces by spin coating a mixture of silica-based oligomer along with single-sized or dual-sized silica particles onto PMMA substrates. The coating film exhibited high mechanical durability and chemical stability due to its identical chemical structures between silica nanoparticles and silica oligomers as well as the formation of covalent Si-O-Si bonding. Three types of coating films (70 nm, 400/70 nm and 650/70 nm) were obtained, where silica-based oligomers were incorporated in the colloidal suspension of silica particles to improve the silica coating adhesion. Among these three types of coatings, the 400/70 nm film was best suited for uniform, transparent, superhydrophobic purposes, while the liquid repellency and optical transparency were compromised on the 70 nm and 650/70 nm films, respectively. Benefiting the identical composition of oligomer binders/silica particles for increased adhesion and physiochemical stability, the dual-sized nanoparticles with hierarchical structures for superhydrophobicity, as well as the high transmittance for optical applications, we envision that our superhydrophobic coating shows great potential for a broad range of applications in medical, solar cell, automobile industries.

Supplementary Material

Refer to Web version on PubMed Central for supplementary material.

Acknowledgments

This project was supported by the LSU Department of Mechanical & Industrial Engineering, the Roy O. Martin Jr. Lumber Co. Professorship of Mechanical Engineering, the National Institute of Biomedical Imaging and Bioengineering of the National Institutes of Health through a research grant R01-EB-010087 and a Biotechnology Resource Center Grant P41-EB-020594, and the State of Louisiana Board of Regents Enhancement Program (LEQSF(2006-07)-ENH-TR-20) and the Louisiana Governor’s Biotechnology Initiative.

References

[1]. Nishino T, Meguro M, Nakamae K, Matsushita M, Ueda Y, The lowest surface free energy based on -CF3 alignment, Langmuir 15 (1999) 4321–4323. 10.1021/La981727s.

[2]. Schwickert H, Strobl G, Kimmig M, Molecular dynamics in perfluoro-n-eicosane. I. Solid phase behavior and crystal structures, J. Chem. Phys 95 (1991) 2800–2806. 10.1063/1.460931.

[3]. Hare EF, Shafrin EG, Zisman WA, Properties of films of adsorbed fluorinated acids, J. Phys. Chem (1954). 10.1021/j150513a011.

[4]. L. X, Y. G, V. L, Effects of Fluorine Atoms Amount and Fluorinated Acrylic Chain Length Chemically Attached to Hydroxyl Groups on the Hydrophobic Properties of Cotton Fabrics, Mod. Chem. Appl (2017). 10.4172/2329-6798.1000204.

[5]. H.Y. ;l. &i. ;r&i. ;. Erbil, Transformation of a Simple Plastic into a Superhydrophobic Surface, Science (80-.) 299 (2003) 1377–1380. 10.1126/science.1078365.

[6]. Tadanaga K, Katata N, Minami T, Formation process of super-water-repellent Al2O3 coating films with high transparency by the Sol-Gel method, J. Am. Ceram. Soc (1997). 10.1111/j.1151-2916.1997.tb03253.x.

[7]. Chan CM, Cao GZ, Fong H, Sarikaya M, Nanoindentation and adhesion of sol-gel derived hard coatings on polyester, J. Mater. Res 15 (2000) 148–154. 10.1557/JMR.2000.0025.

[8]. Nakajima A, Fujishima A, Hashimoto K, Watanabe T, Preparation of transparent superhydrophobic boehmite and silica films by sublimation of aluminum acetylacetonate, Adv. Mater (1999). 10.1002/(SICI)1521-4095(199911)11:16<1365::AID-ADMA1365>3.0.CO;2-F.

[9]. Zhao X, Park DS, Choi J, Park S, Soper SA, Murphy MC, Robust, transparent, superhydrophobic coatings using novel hydrophobic/hydrophilic dual-sized silica particles, J. Colloid Interface Sci 574 (2020). 10.1016/j.jcis.2020.04.065.

[10]. Zhao X, Park DS-W, Soper SA, Murphy MC, Microfluidic Gasketless Interconnects Sealed by Superhydrophobic Surfaces, J. Microelectromechanical Syst (2020) 1–6. 10.1109/JMEMS.2020.3000325.

[11]. Zhao X, Park DS, Choi J, Park S, Soper SA, Murphy MC, Flexible-templated imprinting for fluorine-free, omniphobic plastics with re-entrant structures, J. Colloid Interface Sci (2020). 10.1016/j.jcis.2020.10.046.

[12]. De Gennes PG, Wetting: Statics and dynamics, Rev. Mod. Phys (1985). 10.1103/RevModPhys.57.827.

[13]. Quéré D, Non-sticking drops, Reports Prog. Phys 68 (2005) 2495–2532. 10.1088/0034-4885/68/11/R01.

[14]. Karunakaran RG, Lu C, Zhang Z, Yang S, Highly Transparent Superhydrophobic Surfaces from the Coassembly of Nanoparticles (≤100 nm), Langmuir 27 (2011) 4594–4602. 10.1021/la104067c. [PubMed: 21355577]

[15]. Deng X, Mammen L, Zhao Y, Lellig P, Müllen K, Li C, Butt H-J, Vollmer D, Transparent, Thermally Stable and Mechanically Robust Superhydrophobic Surfaces Made from Porous Silica Capsules, Adv. Mater 23 (2011) 2962–2965. 10.1002/adma.201100410. [PubMed: 21538988]

[16]. Zhang L, Li Y, Sun J, Shen J, Mechanically Stable Antireflection and Antifogging Coatings Fabricated by the Layer-by-Layer Deposition Process and Postcalcination, Langmuir 24 (2008) 10851–10857. 10.1021/la801806r. [PubMed: 18767828]

[17]. Ming W, Wu D, Van Benthem R, De With G, Superhydrophobic films from raspberry-like particles, Nano Lett 5 (2005) 2298–2301. 10.1021/nl0517363. [PubMed: 16277471]

[18]. Athauda TJ, Williams W, Roberts KP, Ozer RR, On the surface roughness and hydrophobicity of dual-size double-layer silica nanoparticles, J. Mater. Sci 48 (2013) 6115–6120.

[19]. Zhao Y, Li J, Hu J, Shu L, Shi X, Fabrication of super-hydrophobic surfaces with long-term stability, J. Dispers. Sci. Technol 32 (2011) 969–974.

[20]. Xiao Y, Huang W, Tsui CP, Wang G, Tang CY, Zhong L, Ultrasonic atomization based fabrication of bio-inspired micro-nano-binary particles for superhydrophobic composite coatings with lotus/petal effect, Compos. Part B Eng 121 (2017) 92–98.

[21]. Zhang H, Tan J, Liu Y, Hou C, Ma Y, Gu J, Zhang B, Zhang H, Zhang Q, Design and fabrication of robust, rapid self-healable, superamphiphobic coatings by a liquid-repellent “glue+ particles” approach, Mater. Des 135 (2017) 16–25.

[22]. Polizos G, Jang GG, Smith DB, List FA, Lassiter MG, Park J, Datskos PG, Transparent superhydrophobic surfaces using a spray coating process, Sol. Energy Mater. Sol. Cells 176 (2018) 405–410.

[23]. Schaeffer DA, Polizos G, Smith DB, Lee DF, Hunter SR, Datskos PG, Optically transparent and environmentally durable superhydrophobic coating based on functionalized SiO2 nanoparticles, Nanotechnology 26 (2015) 55602.

[24]. Gu J, Zhang Q, Li H, Tang Y-S, Kong J, Dang J, Study on preparation of SiO2/epoxy resin hybrid materials by means of sol-gel, Polym. Plast. Technol. Eng 46 (2007) 1129–1134.

[25]. Latthe SS, Sutar RS, Kodag VS, Bhosale AK, Kumar AM, Sadasivuni KK, Xing R, Liu S, Self–cleaning superhydrophobic coatings: Potential industrial applications, Prog. Org. Coatings 128 (2019) 52–58.

[26]. Li X, Li B, Li Y, Sun J, Nonfluorinated, transparent, and spontaneous self-healing superhydrophobic coatings enabled by supramolecular polymers, Chem. Eng. J 404 (2021) 126504.

[27]. Ling XY, Phang IY, Vancso GJ, Huskens J, Reinhoudt DN, Stable and Transparent Superhydrophobic Nanoparticle Films, Langmuir 25 (2009) 3260–3263. 10.1021/la8040715. [PubMed: 19437727]

[28]. He Z, Ma M, Lan X, Chen F, Wang K, Deng H, Zhang Q, Fu Q, Fabrication of a transparent superamphiphobic coating with improved stability, Soft Matter 7 (2011) 6435–6443.

[29]. Feng D, Weng D, Wang J, Interfacial tension gradient driven self-assembly of binary colloidal particles for fabrication of superhydrophobic porous films, J. Colloid Interface Sci 548 (2019) 312–321. [PubMed: 31009849]

[30]. Stöber W, Fink A, Bohn E, Controlled growth of monodisperse silica spheres in the micron size range, J. Colloid Interface Sci 26 (1968) 62–69. 10.1016/0021-9797(68)90272-5.

[31]. Solař P, Polonskyi O, Olbricht A, Hinz A, Shelemin A, Kylián O, Choukourov A, Faupel F, Biederman H, Single-step generation of metal-plasma polymer multicore@ shell nanoparticles from the gas phase, Sci. Rep 7 (2017) 1–6. [PubMed: 28127051]

[32]. Kuzminova A, Shelemin A, Kylián O, Petr M, Kratochvíl J, Solař P, Biederman H, From super-hydrophilic to super-hydrophobic surfaces using plasma polymerization combined with gas aggregation source of nanoparticles, Vacuum 110 (2014) 58–61.

[33]. Favia P, d'Agostino R, Fracassi F, Plasma and surface diagnostics in PECVD (plasma-enhanced chemical vapor deposition) from silicon containing organic monomers, Pure Appl. Chem 66 (1994) 1373–1380.

[34]. Zhao X, Khandoker MAR, Golovin K, Non-Fluorinated Omniphobic Paper with Ultralow Contact Angle Hysteresis, ACS Appl. Mater. Interfaces 12 (2020) 15748–15756. 10.1021/acsami.0c01678. [PubMed: 32142254]

[35]. Li Y, Zhang J, Zhu S, Dong H, Jia F, Wang Z, Sun Z, Zhang L, Li Y, Li H, Xu W, Yang B, Biomimetic surfaces for high-performance optics, Adv. Mater 21 (2009) 4731–4734. 10.1002/adma.200901335.

[36]. Malitson IH, Interspecimen Comparison of the Refractive Index of Fused Silica*,†, J. Opt. Soc. Am 55 (1965) 1205. 10.1364/JOSA.55.001205.

[37]. Schneider PM, Fowler WB, Band structure and optical properties of silicon dioxide, Phys. Rev. Lett 36 (1976) 425–428. 10.1103/PhysRevLett.36.425.

[38]. Vazquez G, Alvarez E, Navaza JM, Surface Tension of Alcohol Water + Water from 20 to 50 .degree.C, J. Chem. Eng. Data 40 (1995) 611–614. 10.1021/je00019a016.

[39]. ISO, Paints and varnishes - Pull-off test for adhesion (ISO 4624:2002), Int. Satandar ISO. (2002).

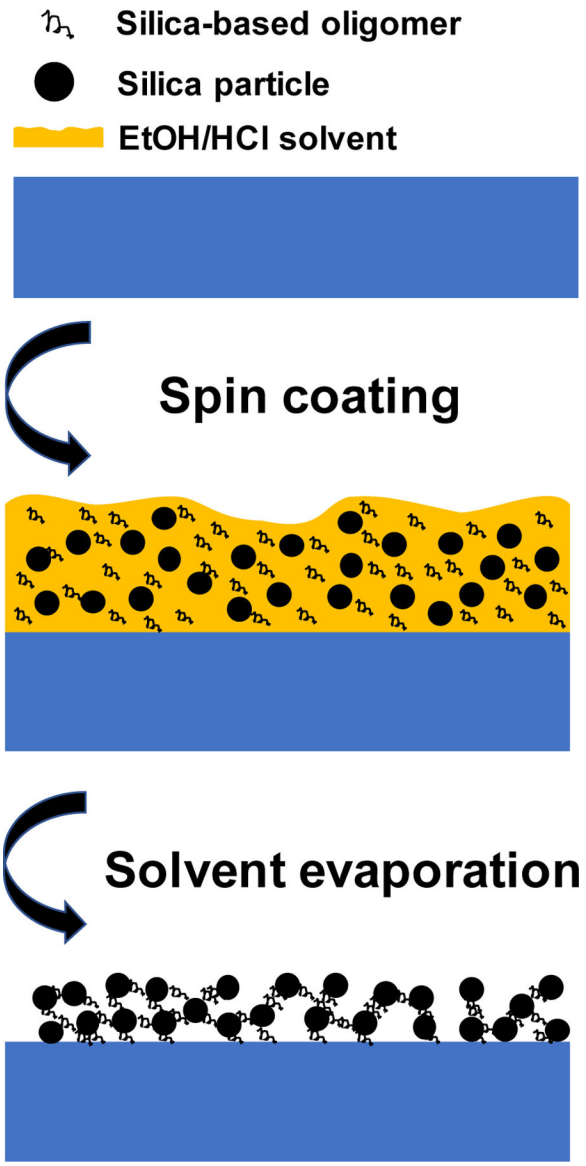

Figure 1.
The schematics showing the spin coating and solvent evaporation of a mixture of silica-based oligomer and silica particles onto PMMA substrates.

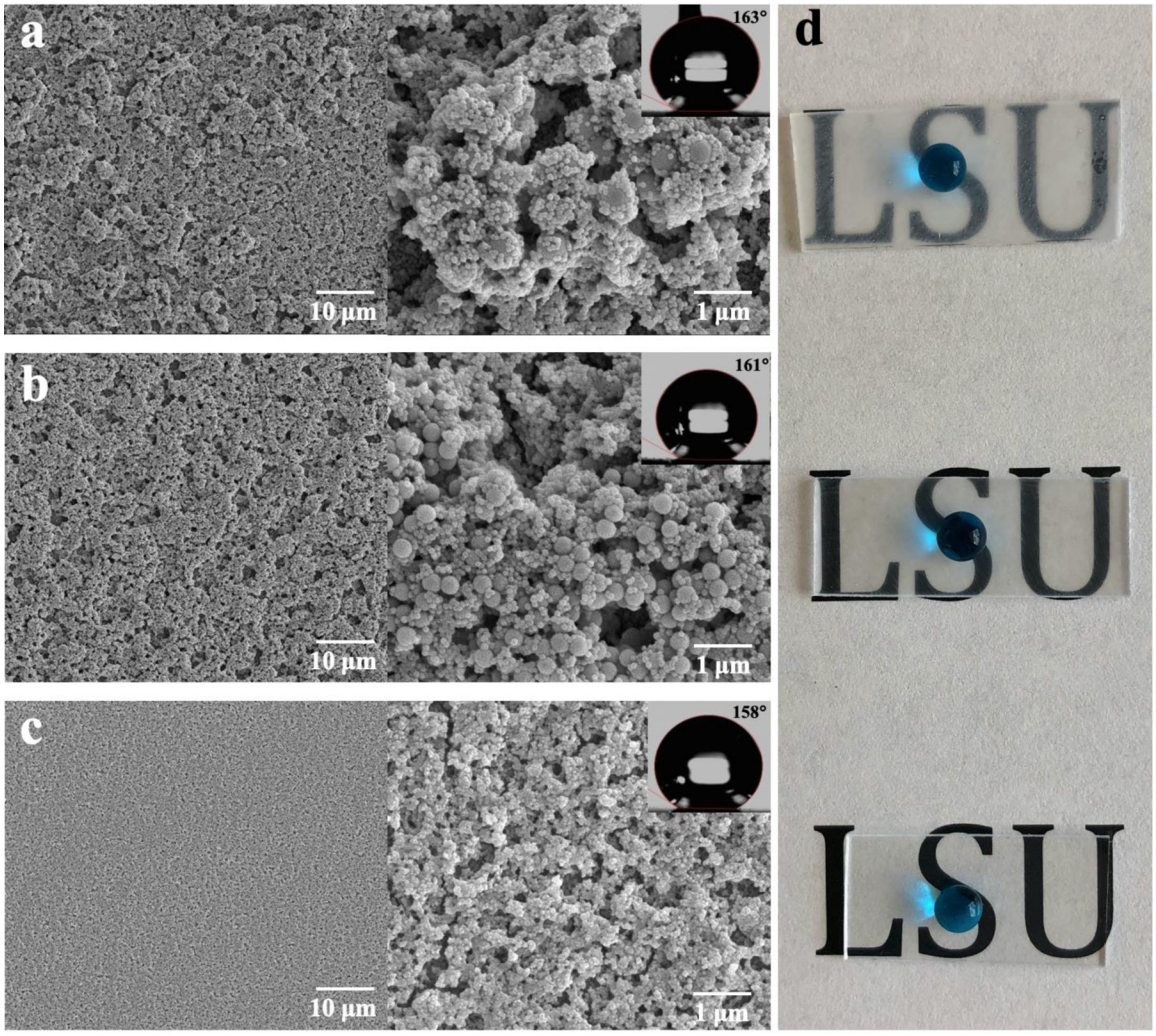

Figure 2.
SEM images of (a) 650/70 nm, (b) 400/70 nm and (c) 70 nm silica films on PMMA substrates, corresponding to (d) the upper, middle, and bottom PMMA substrate of the image.

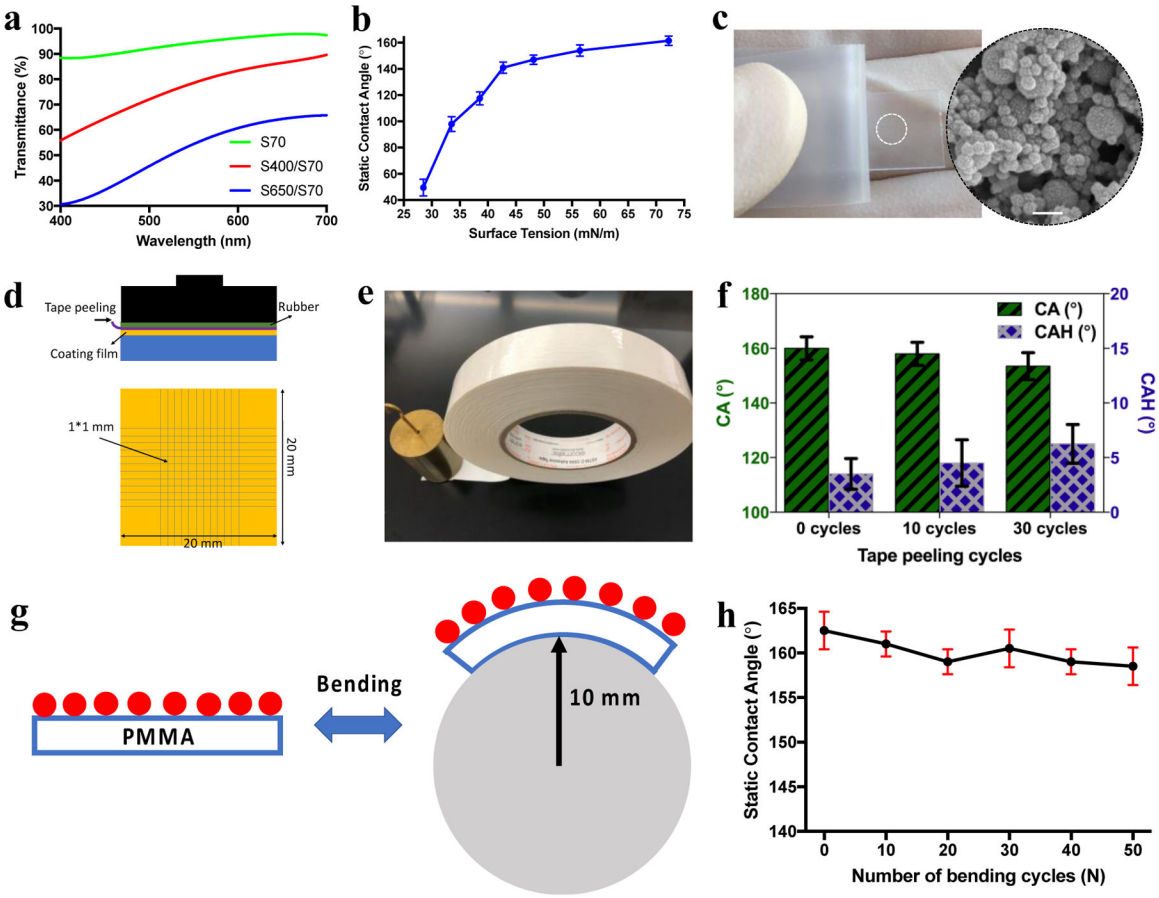

Figure 3.

(a) Transmittance spectra in visible wavelength for 70 nm, 400/70 nm, and 650/70 nm films on PMMA substrates. The graph shows the transmittance percentage with respect to the pristine PMMA. (b) Static CAs for droplets with different surface tensions deposited on the 400/70 nm superhydrophobic coating. (c) Peeling-off test using scotch tape. (d, e) The adhesion force measurement of the silica coating using a standard ISO-2049:2013 cross-cut tape test. (f) The water contact angles and contact angle hysteresis of 400/70 nm coating films after 0, 10, and 30 cycles of tape peeling tests. (g) 400/70 nm coated PMMA substrate under bending with bending radius of 10 mm. (h) Water contact angle as a function of the number of bending cycles for 400/70 nm film.

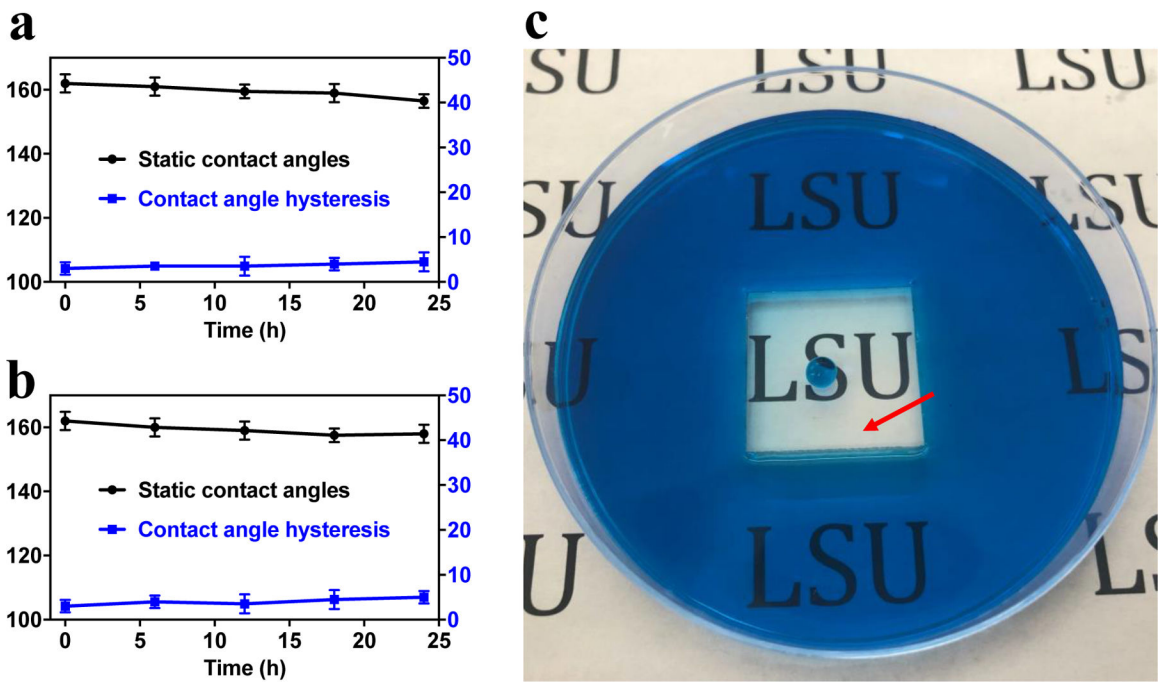

Figure 4.

The PMMA substrates coated with 400/70 nm films were immersed in (a) hydrochloride acid (PH=2) and (b) sodium hydroxide (PH=12) solution and magnetically stirred for up to 24 hours. (c) The coating of superhydrophobic square area in the bottom of a petri dish, and this area remained dry with acidic or basic solution surrounded for 7 days.

Table 1.

Chemical compositions for the preparation of different size of silica nanoparticles.

Silica size/nm Nominal size	Silica size/nm Measured size	Ethanol/mL	Ammonia/mL	TEOS/mL
70	72 ± 29	200	10	5
400	382 ± 68	200	15	7.5
650	658 ± 84	200	20	10